MOX-Report No. 39/2018

Density-based inverse homogenization with anisotropically adapted elements

Ferro, N.; Micheletti, S.; Perotto, S.

MOX, Dipartimento di Matematica
Politecnico di Milano, Via Bonardi 9 - 20133 Milano (Italy)

mox-dmat@polimi.it http://mox.polimi.it

Density-based inverse homogenization with anisotropically adapted elements

Nicola Ferro[#], Stefano Micheletti[#], Simona Perotto[#]

June 22, 2018

[#] MOX– Modellistica e Calcolo Scientifico
Dipartimento di Matematica, Politecnico di Milano
Piazza L. da Vinci 32, I-20133 Milano, Italy
{nicola.ferro,stefano.micheletti,simona.perotto}@polimi.it

Abstract

The optimization of manufacturable extremal elastic materials can be carried out via topology optimization using the homogenization method. We combine here a standard density-based inverse homogenization technique with an anisotropic mesh adaptation procedure in the context of a finite element discretization. In this way, the optimized layouts are intrinsically smooth and ready to be manufactured.

1 Introduction

The design of performant and light structures has been gaining popularity for the last years thanks to the rise and development of Additive Manufacturing (AM) techniques. Differently from subtractive methods, AM enjoys great versatility in the achievable shapes and presents very few limitations.

In this framework, topology optimization (TO) has proved to be the reference mathematical method suitable for designing innovative and performant structures of engineering interest. Essentially, it consists in the allocation of material in the so-called design domain, ensuring the optimization of a given functional and, at the same time, the satisfaction of design requirements. The final result of TO is an optimized structure, where areas of full material and void alternate so that the new topology guarantees the desired production specifications.

With a particular focus on the linear elastic problem, it is observed that the stiffness of an optimal designed structure, subject to given loads and constraints, is increased by inserting small substructures [2]. Consequently, different authors have investigated the possibility of employing topology optimization at a microscale as well, aiming at yielding optimized microstructures (metamaterials)

[24, 26]. The ultimate goal is to combine the microscopic optimized structures with a standard TO performed at the macroscale. This link is made possible by employing homogenization techniques, which are widely used to incorporate the information provided by the microscale into macroscale models [1, 3, 20].

In this work, we enrich such an approach by resorting to a numerical discretization of the linear elastic problem based on a standard finite element solver combined with a mesh adaptation procedure. In particular, in Section 2, we briefly present a density-based approach for a generic topology optimization problem. In Section 3, the homogenization procedure is presented. We distinguish between a direct and an inverse method, consisting in prescribing the desired macroscopic effective values in order to retrieve the optimal microstructure. Section 4 is devoted to the numerical approximation and to the anisotropic setting used for the finite element discretization. In particular, we examine the mathematical tool employed to anisotropically adapt a two-dimensional mesh to the problem at hand, coupling such a procedure with the inverse homogenization technique. In Section 5, some numerical results are provided in order to assess the proposed algorithm, and finally some conclusions are drawn in Section 6.

2 A density-based method for topology optimization

We consider the SIMP formulation for topology optimization to address the structural optimization problem [2]. In this context, the optimal layout of a material is determined in terms of an auxiliary scalar field, say ρ, defined over the domain Ω. In particular, ρ is a relative density belonging to $L^\infty(\Omega, [0,1])$, determining presence of full material ($\rho = 1$) or void ($\rho = 0$). The optimization problem is set once the objective function $\mathcal{C}$ and the design requirements are defined, while a balance equation $\mathcal{S}$ constrains the optimization. Then, in order to account for changes in the topology, the state equation $\mathcal{S}$ is properly modified to include the density variable in the formulation. The final optimization problem thus reads

$$\min_{\rho \in L^\infty(\Omega)} \mathcal{C}(\rho) \; : \begin{cases} \text{State equation } \mathcal{S}(\rho) \text{ is satisfied} \\ \text{Boundary conditions} \\ \int_\Omega \rho \, d\Omega \; \leq \alpha |\Omega| \\ \rho_{\min} \leq \rho \leq 1, \end{cases} \tag{1}$$

where α is the maximum volume fraction we wish to ensure in the final configuration, and $\rho_{\min}$ is a lower bound for the density, to avoid the possible ill-posedness of $\mathcal{S}$.

In particular, $\mathcal{S}$ is chosen accordingly to the physical phenomenon under investigation, i.e., to the application at hand. For instance, for the optimization of elastic structures, the state equation can be represented by the linear elastic equation, whereas, when considering the optimization of the energy dissipation of a steady flow, one can identify $\mathcal{S}$ with the Stokes equations. In the specific

case of the present work, we deal with the optimization of the design of elastic microstructures. A homogenized version of the elastic equations will represent the reference state equation as detailed in the following section. Concerning the inclusion of the density variable in the state equation, a suitable power law of ρ is usually employed to weight the main physical constants in $\mathcal{S}$, such as the standard Lamé constants, λ and μ, for the elastic problem or the inverse permeability of the fluid for the Stokes equations.

3 The homogenization procedure

The homogenization method is an asymptotic technique whose goal is to assign macroscopic effective properties to microscopic entities, which are arranged periodically. This approach plays a crucial role in multiscale simulations since it allows one to deal with the macroscale only, the effects of the microscale being inherited through homogenization. The technique has been widely investigated both theoretically [3, 20] and numerically [1], and it is a well-established practice.

In this section, we analyze also the converse technique, known as inverse homogenization [14, 19, 21, 22]. This can be formulated as a control problem or, specifically, as a topology optimization problem. The aim is to find the optimal arrangement of material at the microscale so that desired effective properties are guaranteed at the macroscale. Notice that the flow of information is opposite with respect to the classical homogenization. The macroscale is fixed or prescribed, whereas the microscale is modified to match the desired requirements.

3.1 The direct method

Direct homogenization has been employed in different fields of application to modify the macroscale model according to the microscale layout [6, 12, 20]. This technique relies on the periodic arrangement of a microstructure which constitutes the base cell, Y. Such elementary entity represents the domain of interest and it is analyzed in order to retrieve its effect on the macroscale.

Let us consider the linear elasticity equation [11]

$$-\nabla \cdot \sigma(\mathbf{u}) = \mathbf{f} \quad \text{in } \Omega, \tag{2}$$

where $\Omega \subset \mathbb{R}^2$ is the domain under investigation at the macroscale, $\mathbf{f}$ is the volumetric forcing term, $\mathbf{u} = [u_1, u_2]^T$ is the displacement field, and σ is the stress tensor. For the sake of generality, we stick to the convention of denoting by E_{ijkl} the fourth-order stiffness tensor, so that the stress tensor has components

$$\sigma_{ij} = E_{ijkl}\varepsilon_{kl} \text{ with } \varepsilon_{kl} = \frac{1}{2}\left(\frac{\partial u_k}{\partial x_l} + \frac{\partial u_l}{\partial x_k}\right),$$

where x_l, with $l = 1, 2$, are the spatial coordinates, ε_{kl} are the components of the strain tensor ε, and we have adopted the Einstein notation to manage index summation.

The homogenization technique relies on the repetition of the base cell Y. In order to preserve this physical feature, we impose periodic boundary conditions. In this way, we enforce that the displacement field $\mathbf{u}$ is equal in correspondence with opposite boundaries [5].

Then, the actual objective becomes to compute the homogenized (or effective) stiffness tensor, E^H, representing a macroscopic mean value of the tensor E, after neglecting the microscale fluctuations E^*. To this end, we resort to an asymptotic expansion of the displacement field $\mathbf{u}$ with respect to the base cell size, considering only the first two terms. Then, following [3, 21], it can be shown that the homogenized tensor E^H is given by

$$E^H_{ijkl} = \frac{1}{|Y|} \int_Y E_{ijpq}(\varepsilon^{0,kl}_{pq} - \varepsilon^{*,kl}_{pq})\, dY, \tag{3}$$

where $|Y|$ is the measure of the cell Y, $\varepsilon^{0,kl}$ identifies a fixed strain field, chosen among the four linearly independent possible fields (k, l being equal to $1, 2$), while $\varepsilon^{*,kl}$ is the Y-periodic fluctuation strain, i.e., the weak solution to the equation

$$\int_Y E_{ijpq}\varepsilon^{*,kl}_{pq}\varepsilon_{ij}(v)\, dY = \int_Y E_{ijpq}\varepsilon^{0,kl}_{pq}\varepsilon_{ij}(v)\, dY, \quad \forall v \in V, \tag{4}$$

$V \subset [H^1(Y)]^4$ being a periodic Sobolev function space. Thus, by combining (3) and (4), we obtain the final form of the effective stiffness tensor [1, 21]

$$E^H_{ijkl} = \frac{1}{|Y|} \int_Y E_{pqrs}(\varepsilon^{0,kl}_{pq} - \varepsilon^{*,kl}_{pq})(\varepsilon^{0,ij}_{rs} - \varepsilon^{*,ij}_{rs})\, dY. \tag{5}$$

Equations (4) and (5) constitute the state equations to be employed in the inverse homogenization technique, as detailed in the following section.

3.2 The inverse method

We refer to inverse homogenization as to the procedure concerning the design of a base cell, Y, whose contribution to the macroscale, according to the direct homogenization process in the previous section, is prescribed [19, 22]. In order to modify the formulation of the direct method, we have to account for variations in the initial distribution of material in the base cell. This goal can be pursued via topology optimization, yielding optimized structures according to specific, user-defined, constraints and objectives.

The same paradigm as in Section 2 is now exploited to incorporate the cell design in the homogenization problem. Let us fix the objective function, $\mathcal{J}$, as a control over the quadratic deviation between the computed value of the homogenized stiffness tensor, E^H, and the requested one, E^W, i.e.,

$$\mathcal{J} = \sum_{ijkl} (E^H_{ijkl}(\rho) - E^W_{ijkl})^2.$$

Hence, the minimization of $\mathcal{J}$ should lead to a micro-design, whose macro-features are the ones desired by the user [22]. Thus, the final system for the micro-optimization is obtained by solving the following problem

$$\min_{\rho \in L^\infty(Y)} \mathcal{J}(\rho) \ : \begin{cases} (4)_\rho - (5)_\rho \text{ are satisfied} \\ + \text{ Periodicity conditions} \\ \int_Y \rho \, dY \ \leq \alpha |Y| \\ \rho_{\min} \leq \rho \leq 1, \end{cases} \tag{6}$$

where $(4)_\rho - (5)_\rho$ represent equations (4) and (5) after replacing E_{ijkl} with $\rho^p E_{ijkl}$, in order to include the design variable ρ in the formulation, p being a penalization exponent.

4 The numerical discretization

Problem (6) can be numerically solved via a finite element discretization [7]. After introducing a conforming tessellation $\mathcal{T}_h = \{K\}$ of Y, with K the generic triangle, we denote by V_h^r the associated finite element spaces of piecewise polynomials of degree $r > 0$, with h the maximum diameter of the mesh elements.

The topology optimization problem discretized via a finite element scheme is known to suffer from several numerical issues [15, 23]. Some of these can be tackled with a suitable choice of the spaces employed to discretize displacement and density or via filtering techniques. Here, we propose to contain any post-processing phase by exploiting the intrinsic smoothness of the optimized density field yielded using ad-hoc meshes. In particular, we choose to discretize problem (6) on a sequence of anisotropically adapted grids and, consequently, we modify the optimization algorithm to deliver smooth and, essentially, directly manufacturable structures.

4.1 The anisotropic setting

We resort to an anisotropic adaptive procedure driven by the density field ρ, which is expected to sharply change from 0 to 1 in correspondence with the boundaries of the structure. The expected strong gradients across the material-void interface justify the employment of anisotropic meshes as an ideal tool to sharply describe the directional features of the density field.

We follow a metric-based procedure in order to generate the optimal mesh to discretize the problem [10]. Essentially, the adaptation procedure relies on an a posteriori error estimator, merging the error information with the geometric properties of the grid. In particular, we employ an anisotropic variant of the Zienkiewicz-Zhu estimator [25], to evaluate the H^1-seminorm of the discretization error, which is expected to be the most effective measure for detecting the material-void interface. Following [16], the elementwise contribution to the

anisotropic error estimator is

$$\eta_K^2 = \frac{1}{\lambda_{1,K}\lambda_{2,K}} \sum_{i=1}^{2} \lambda_{i,K}^2 \left(\mathbf{r}_{i,K}^T \, G_{\Delta_K}(E_\nabla) \mathbf{r}_{i,K} \right), \tag{7}$$

where $\lambda_{1,K}$ and $\lambda_{2,K}$ are the lengths of the semi-axes of the ellipse circumscribed to element K, while $\mathbf{r}_{1,K}$ and $\mathbf{r}_{2,K}$ represent the directions of such axes. The quantity $E_\nabla = \left[P(\nabla\rho_h) - \nabla\rho_h\right]_{\Delta_K}$ is the recovered error associated with the density ρ, where $P(\nabla\rho_h)|_{\Delta_K} = |\Delta_K|^{-1} \sum_{T\in\Delta_K} |T| \nabla\rho_h|_T$ denotes the recovered gradient computed on the patch Δ_K of the elements sharing at least a vertex with K, $|\cdot|$ being the measure operator, and $\nabla\rho_h$ is the gradient of the discrete density [9, 17]. Finally, $G_{\Delta_K}(\cdot) \in \mathbb{R}^{2\times 2}$ is the symmetric positive semidefinite matrix with entries

$$[G_{\Delta_K}(\mathbf{w})]_{i,j} = \sum_{T\in\Delta_K} \int_T w_i \, w_j \, dT \quad \text{with } i,j = 1,2, \tag{8}$$

for any vector-valued function $\mathbf{w} = (w_1, w_2)^T \in [L^2(\Omega)]^2$. Then, the global error estimator is given by $\eta^2 = \sum_{K\in\mathcal{T}_h} \eta_K^2$.

The mesh adaptation is carried out by minimizing the number of elements of the adapted mesh, while requiring an upper bound `TOLAD` to the global error estimator η together with an error equidistribution criterion. This gives rise to an elementwise constrained optimization problem which admits a unique analytic solution. Specifically, by introducing the aspect ratio $s_K = \lambda_{1,K}/\lambda_{2,K} \geq 1$ measuring the deformation of element K, the adapted grid is characterized by the following quantities

$$s_K^{adapt} = \sqrt{g_1/g_2}, \quad \mathbf{r}_{1,K}^{adapt} = \mathbf{g}_2, \quad \mathbf{r}_{2,K}^{adapt} = \mathbf{g}_1,$$

where $\{g_i, \mathbf{g}_i\}_{i=1,2}$ are the eigen-pairs associated with the scaled matrix $\widehat{G}_{\Delta_K}(E_\nabla) = G_{\Delta_K}(E_\nabla)/|\Delta_K|$, with $g_1 \geq g_2 > 0$, $\{\mathbf{g}_i\}_{i=1,2}$ orthonormal vectors.
Finally, imposing the equidistribution, i.e., $\eta_K^2 = \texttt{TOLAD}^2/\#\mathcal{T}_h$, with $\#\mathcal{T}_h$ the mesh cardinality, we obtain the geometric information identifying the new adapted mesh, i.e.,

$$\lambda_{1,K}^{adapt} = g_2^{-1/2} \left(\frac{\texttt{TOLAD}^2}{2\#\mathcal{T}_h \, |\widehat{\Delta}_K|} \right)^{1/2}, \quad \lambda_{2,K}^{adapt} = g_1^{-1/2} \left(\frac{\texttt{TOLAD}^2}{2\#\mathcal{T}_h \, |\widehat{\Delta}_K|} \right)^{1/2}, \tag{9}$$
$$\mathbf{r}_{1,K}^{adapt} = \mathbf{g}_2, \quad \mathbf{r}_{2,K}^{adapt} = \mathbf{g}_1,$$

with $|\widehat{\Delta}_K| = |\Delta_K|/(\lambda_{1,K}\lambda_{2,K})$.

4.2 The adaptive algorithm

The algorithm employed to merge the topology optimization of the base cell Y with the mesh adaptation procedure described above is here presented. We name it microSIMPATY algorithm since it is inspired to the algorithm SIMPATY in [18].

Algorithm 1 : microSIMPATY

Input : $\texttt{CTOL}, \texttt{TOLAD}, \texttt{TOPT}, \texttt{kmax}, \rho_{\min}, \mathcal{T}_h^{(0)}$

1: Set: ρ_h^0, k = 0, errC = 1 + CTOL
2: **while** errC > CTOL & k < kmax **do**
3: $\quad \rho_h^{k+1} = \texttt{optimize}(\rho_h^k, \texttt{Mit}, \texttt{TOPT}, \rho_{\min}, \mathcal{J}(\rho), \nabla_\rho \mathcal{J}(\rho), ...)$;
4: $\quad \mathcal{T}_h^{(k+1)} = \texttt{adapt}(\mathcal{T}_h^{(k)}, \rho_h^{k+1}, \texttt{TOLAD})$;
5: $\quad$ errC = $|\#\mathcal{T}_h^{(k+1)} - \#\mathcal{T}_h^{(k)}|/\#\mathcal{T}_h^{(k)}$;
6: **end while**

In Algorithm 1, `optimize` is a numerical routine for the inverse topology optimization, which stops whenever the maximum number of iterations, `Mit`, is exceeded, or the prescribed tolerance, `TOPT`, is satisfied. Beside the objective function $\mathcal{J}(\rho)$, the corresponding derivative with respect to ρ is required by the `optimize` algorithm, as well as other possible constraints to be imposed, with the associated derivatives. Such sensitivities are analytically computed following a Lagrangian approach [4]. Function `adapt` is a routine performing the mesh adaptation starting from the metric derived in (9). The algorithm is terminated by two stopping criteria, one based on the number of iterations, the other on the stagnation of the number of elements between two consecutive mesh adaptations to within `CTOL`.

5 Numerical results

The following numerical verification has been carried out with `FreeFem++` [13], which provides the users with built-in functions for both optimization [8] and metric-based mesh adaptation. In both the considered test cases, we deal with the design of a 1[m] $\times$1[m] base cell with negative Poisson ratio $\nu = \lambda/[2(\lambda+\mu)]$, corresponding to E_{1122}. We choose $p = 4$ for the penalization exponent in (6). The material employed has Young modulus equal to 0.91[Pa] and Poisson ratio $\nu = 0.3$. Finally, ρ_h^0 is set to $|\sin(2\pi x_1)\sin(2\pi x_2)|$.

Case 1. In Figure 1, the results for $E^W_{1122} = -1$ are shown. We require a volume fraction $\alpha = 0.3$, we start with an initial structured mesh consisting of 1800 elements, and we pick $\texttt{TOLAD} = 10^{-5}$, $\texttt{CTOL} = 10^{-4}$, $\texttt{TOPT} = 10^{-3}$, $\rho_{\min} = 10^{-4}$, $\texttt{kmax} = 20$, while the maximum number of iterations, `Mit`, is set to 35 for the first three iterations and to 10 for the next ones. The algorithm stops

after 20 iterations, delivering a structure with $E^H_{1122} = -0.65$. The final design

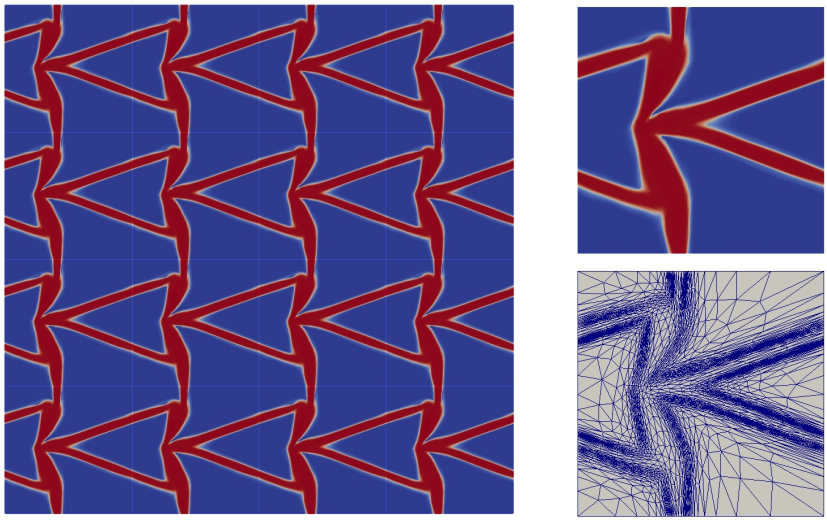

Figure 1: Optimized microstructure for $E^W_{1122} = -1$: 4×4 periodic arrangement of the base cell (left), base cell (top-right) and corresponding adapted mesh (bottom-right).

thus obtained is comparable with the one in [14], Figure 3, while the quality of the solution is increased when resorting to the microSIMPATY algorithm, no filtering techniques being required. In Figure 1, bottom-right, we show the last adapted grid. Notice that the elements are highly stretched and concentrated in correspondence with the void-solid interface. The cardinality of such final mesh is 2620 and its maximum aspect ratio is 97.76.

Case 2. The second case concerns the optimization of a micro-design with $E^W_{1122} = -0.7$ and $\alpha = 0.5$ (see [21], Figure 2.17). As for the previous test, we perform 20 iterations, starting from a structured mesh of 1800 elements and picking the same parameters as in the previous case, except for `Mit`, which is now set to 35 at the first iteration, to 25 until the fifth one, and to 15 for the later iterations. The results in Figure 2 show a very smooth solution, where intermediate densities are very limited to a thin boundary layer, whose quality is enhanced by the adapted grid. In the final mesh, the directionalities of the density field are properly detected, making 4266 elements enough for a sharply-defined solution, with a maximum value for the aspect ratio equal to 85.58. The final structure delivers an effective Poisson ratio equal to -0.54.

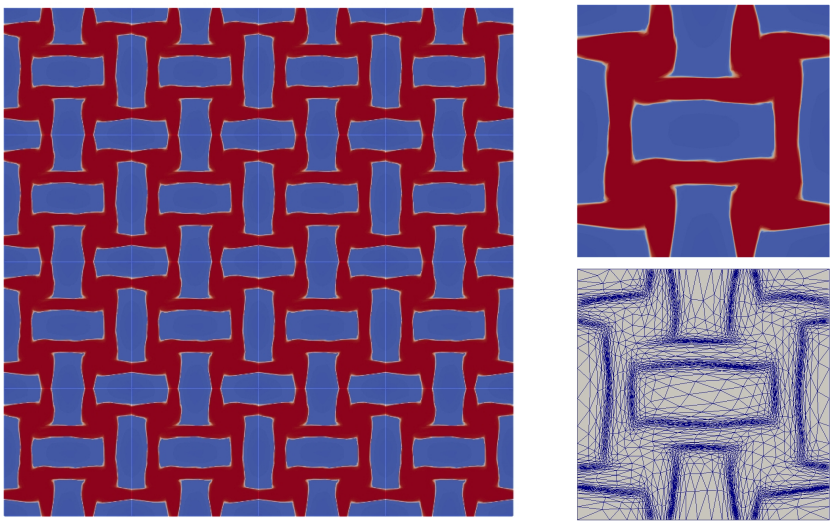

Figure 2: Optimized microstructure for $E^W_{1122} = -0.7$: 4×4 periodic arrangement of the base cell (left), base cell (top-right) and corresponding adapted mesh (bottom-right).

6 Conclusions

In this work, we presented an algorithm to optimize microstructures according to user-defined requirements, based on the inverse homogenization method, properly merged with an anisotropic mesh adaptation procedure.

The structures derived in Section 5 are consistent with the ones available in the literature and exhibit a remarkable smoothness along structure boundaries, the thin material/void layers being sharply detected by the adapted mesh. This feature confirms the benefits due to microSIMPATY algorithm.

Nevertheless, the optimization process depends on several parameters to be accurately tuned in order to meet user requirements. For this reason, we plan to perform a more rigorous investigation in such a direction, especially to make the homogenized stiffness tensor closer to the requested one.

Finally, with a view to real applications, we are extending the algorithm to a 3D framework.

References

[1] Andreassen, E., Andreasen, C.S.: How to determine composite material properties using numerical homogenization. Comp. Mater. Sci. **83**, 488–495 (2014)

[2] Bendsøe, M.P., Sigmund, O.: Topology Optimization – Theory, Methods and Applications. Springer-Verlag, Berlin (2003)

[3] Bensoussan, A., Lions, J.L., Papanicolaou, G.: Asymptotic Analysis for Periodic Structures. AMS Chelsea Publishing, Providence, RI (2011)

[4] Bertsekas, D.P.: Constrained Optimization and Lagrange Multiplier Methods. Computer Science and Applied Mathematics. Academic Press, Inc., New York-London (1982)

[5] Brezis, H.: Functional Analysis, Sobolev Spaces and Partial Differential Equations. Universitext. Springer, New York (2011)

[6] Chung, P.W., Tamma, K.K., Namburu, R.R.: Homogenization of temperature-dependent thermal conductivity in composite materials. J. Thermophys. Heat Tr. **15**(1), 10–17 (2001)

[7] Ciarlet, P.G.: The Finite Element Method for Elliptic Problems. North-Holland Publishing Co., Amsterdam-New York-Oxford (1978)

[8] Curtis, F.E., Schenk, O., Wächter, A.: An interior-point algorithm for large-scale nonlinear optimization with inexact step computations. SIAM J. Sci. Comput. **32**(6), 3447–3475 (2010)

[9] Farrell, P.E., Micheletti, S., Perotto, S.: An anisotropic Zienkiewicz-Zhu-type error estimator for 3D applications. Internat. J. Numer. Methods Engrg. **85**(6), 671–692 (2011)

[10] Frey, P.J., George, P.L.: Mesh Generation: Application to Finite Elements. Wiley Online Library (2008)

[11] Gould, P.L.: Introduction to Linear Elasticity. Springer, Paris (1994)

[12] Hashin, Z., Shtrikman, S.: A variational approach to the theory of the effective magnetic permeability of multiphase materials. J. Appl. Phys. **33**(10), 3125–3131 (1962)

[13] Hecht, F.: New development in freefem++. J. Numer. Math. **20**(3-4), 251–266 (2012)

[14] Larsen, U.D., Signund, O., Bouwsta, S.: Design and fabrication of compliant micromechanisms and structures with negative Poisson's ratio. J. Microelectromech. S. **6**(2), 99–106 (1997)

[15] Lazarov, B.S., Sigmund, O.: Filters in topology optimization based on Helmholtz-type differential equations. Internat. J. Numer. Methods Engrg. **86**(6), 765–781 (2011)

[16] Micheletti, S., Perotto, S.: Anisotropic adaptation via a Zienkiewicz–Zhu error estimator for 2D elliptic problems. In: G. Kreiss, P. Lötstedt, A. Målqvist, M. Neytcheva (eds.) Numerical Mathematics and Advanced Applications, pp. 645–653. Springer-Verlag Berlin Heidelberg, Berlin, Heidelberg (2010)

[17] Micheletti, S., Perotto, S., Farrell, P.E.: A recovery-based error estimator for anisotropic mesh adaptation in CFD. Bol. Soc. Esp. Mat. Apl. SeMA (50), 115–137 (2010)

[18] Micheletti, S., Perotto, S., Soli, L.: Ottimizzazione topologica adattativa per la fabbricazione stratificata additiva (2017). Italian patent application No. 102016000118131, filed on November 22, 2016 (extended as *Adaptive topology optimization for additive layer manufacturing*, International patent application PCT No. PCT/IB2017/057323)

[19] Neves, M.M., Rodrigues, H., Guedes, J.M.: Optimal design of periodic linear elastic microstructures. Comput. Struct. **76**(1-3), 421–429 (2000)

[20] Sánchez-Palencia, E.: Homogenization Method for the Study of Composite Media. In: Asymptotic analysis, II, *Lecture Notes in Math.*, vol. 985, pp. 192–214. Springer, Berlin-New York (1983)

[21] Sigmund, O.: Design of Material Structures Using Topology Optimization. Technical University of Denmark, Lyngby, Denmark (1994)

[22] Sigmund, O.: Materials with prescribed constitutive parameters: an inverse homogenization problem. Internat. J. Solids Structures **31**(17), 2313–2329 (1994)

[23] Sigmund, O., Petersson, J.: Numerical instabilities in topology optimization: a survey on procedures dealing with checkerboards, mesh-dependencies and local minima. Struct. Multidiscip. O. **16**(1), 68–75 (1998)

[24] Yin, L., Ananthasuresh, G.: Topology optimization of compliant mechanisms with multiple materials using a peak function material interpolation scheme. Struct. Multidiscip. O. **23**(1), 49–62 (2001)

[25] Zienkiewicz, O.C., Zhu, J.Z.: A simple error estimator and adaptive procedure for practical engineerng analysis. Int. J. Numer. Meth. Eng. **24**(2), 337–357 (1987)

[26] Zuo, W., Saitou, K.: Multi-material topology optimization using ordered SIMP interpolation. Structural and Multidisciplinary Optimization **55**(2), 477–491 (2017)

MOX Technical Reports, last issues

Dipartimento di Matematica
Politecnico di Milano, Via Bonardi 9 - 20133 Milano (Italy)

38/2018 Domanin, M.; Gallo, D.; Vergara, C.; Biondetti, P.; Forzenigo, L.V.; Morbiducci, U.
Prediction of long term restenosis risk after surgery in the carotid bifurcation by hemodynamic and geometric analysis

37/2018 Bonaventura, L.; Della Rocca A.;
Convergence analysis of a cell centered finite volume diffusion operator on non-orthogonal polyhedral meshes

32/2018 Dal Santo, N.; Deparis, S.; Manzoni, A.; Quarteroni, A.
An algebraic least squares reduced basis method for the solution of nonaffinely parametrized Stokes equations

34/2018 Laurino, F.; Coclite, A.; Tiozzo, A.; Decuzzi, P.; Zunino, P.;
A muliscale computational approach for the interaction of functionalized nanoparticles with the miscrovasculature

35/2018 Possenti, L.; Casagrande, G.; Di Gregorio, S.; Zunino, P.; Costantino, M.L.
Numerical simulations of the microvascular fluid balance with a non-linear model of the lymphatic system

36/2018 Agosti, A.; Ambrosi, D.; Turzi, S.
Strain energy storage and dissipation rate in active cell mechanics

31/2018 Quarteroni, A.
The role of statistics in the era of big data: A computational scientist' perspective

30/2018 Ieva, F.; Palma, F.; Romo, J.
Bootstrap-based Inference for Dependence in Multivariate Functional Data

29/2018 Manzoni, A; Bonomi, D.; Quarteroni, A.
Reduced order modeling for cardiac electrophysiology and mechanics: new methodologies, challenges & perspectives

28/2018 Gerbi, A.; Dede', L.; Quarteroni, A.
Segregated algorithms for the numerical simulation of cardiac electromechanics in the left human ventricle